

## Soil Salinity Monitoring and Quantification Using Modern Techniques

Marwah M. Al-Khuzai<sup>1,2</sup>, Khairul Nizam Abdul Maulud<sup>1,3\*</sup>, Aizat Mohd Taib<sup>1</sup>

<sup>1</sup> Department of Civil Engineering, Faculty of Engineering and Built Environment, Universiti Kebangsaan Malaysia, 43600 UKM Bangi, Selangor, Malaysia

<sup>2</sup> Civil Engineering Department, College of Engineering, University of Al-Qadisiyah, Al-Qadisiyah, Iraq

<sup>3</sup> Earth Observation Centre, Institute of Climate Change, Universiti Kebangsaan Malaysia, 43600 UKM, Bangi, Selangor, Malaysia

\* Corresponding author's e-mail: knam@ukm.edu.my

### ABSTRACT

Along with sea-level rise, one of the most detrimental effects of climate change, is salinity leakage, which significantly affects agricultural activities throughout most of the world. This occurrence is becoming increasingly dangerous. The purpose of this study was to use Geographical Information Systems (GIS) to assess the current situation of agricultural lands in the province of Al-Diwaniyah, by employing GIS to document the salt-affected sites and arrive at the most important criteria affecting those lands as well as build an application model for suitability to clarify the affected sites and come up with paper and digital maps. To accomplish this, the study relied on the available data by extrapolating and analyzing remote sensing images using salt equations to analyze the Landsat 8 satellite images, after which these data were subjected to spatial statistical treatment in ArcGIS software. Moreover, 20 samples were taken from ground sampling points and subjected to laboratory analysis to compare and document the results. The research resulted in the creation of an up-to-date database for the locations of salt ratio growth or decrease in the province of Al-Diwaniyah, which can be relied on, starting from and expanding in the future. Land maps, both paper and digital, have been created and can be used and inferred. The findings demonstrated the model's ability to steadily discriminate among all salinity groups while maintaining consistency with the ground truth data. Each of the four major salinity categories was highlighted. The best-performing indicators were used to build the MLR model, which was then used to anticipate soil salinity. The salt levels may be determined by the MLR combining NDVI and SI-5 with a high correlation value ( $R^2 = 75.29\%$ ). Finally, it is shown that by combining spectral indicators with field measurements, it is possible to chart and forecast soil salinity on a large scale.

**Keywords:** salinity; GIS; soil salinity indicators; regression models.

### INTRODUCTION

The accumulation of salts on the earth or in the surrounding area is shown by soil salinity. (Salin. Environ. - Plants - Mol., 2004) Depletion occurs mostly in arid and semiarid environments, with soil being the primary cause (Jordán et al., 2004). Soil salinity is highly variable and well-regulated throughout the landscape. Parent content, permeability, drainage, and climatic influences (rainfall and humidity) are among these variables (Ben-Dor et al., 2008). The characteristics of soil salinity usually are determined using soil-paste saturation

or water extracts that utilize a spectrometer to determine the electric conductivity (EC) and various soil-to-water ratios (Goldshleger et al., 2013). The density of the soil samples is based on detailed maps a comprehensive architecture that makes the mapping time-intensive and costly requires previous techniques. In the past decades, The salinity of soils has been extensively mapped using remote sensing data, either in real-time and in various sizes, whether bare soils directly or vegetation indirectly (Liang et al., 2019). In addition, several methods have been accompanied by the evaluation of spatial soil salinity modeling using

numeric equations to simulate and forecast actual phenomena and processes. The methods used include a neural artificial network (Akramkhanov and Vlek, 2012), hierarchical classification and regressive tree (Taghizadeh-Mehrjardi et al., 2014) fuzzy analysis (Malins and Metternicht, 2006) a generalization of Bayesian Inference (Douaik et al., 2004) and statistical perception (Eldeiry and Garcia, 2008). A summary of these methods and how they achieve the best outcomes under some conditions (Minasny and McBratney, 2016).

For designing soil prediction models, an adaptive methodology that includes RS, as well as other computational methods, is very promising. Due to its pace, practicability, and cost-effectiveness, statistical analysis, especially linear regression, has provided a considerable potential for change in the way soil salinity is modeled in the case salinity of the soil. (Lesch et al., 1995). In the research literature, the development and use of statistical models based on remote sensing data, with all of them demonstrating the ability to produce reliable salinity predictions (Qu et al., 2008; Wang et al., 2020), based on spectral variables such as the Normalized Difference Salinity Index (NDSI), the Normalized Difference Vegetation Index (NDVI), the initial eight bands of Landsat Enhanced Thematic Mapper plus (Landsat ETM+), and soil characteristics, developed a number of salinity prediction models. The findings revealed that the measured EC had the strongest interaction with have near-infrared (band 4) and the mid-infrared (band 7) wavelengths. The salinity prediction models based on the combination of these variables may be used to estimate soil salinity over a wide region. It was discovered that of the Landsat ETM+ bands (1–5) and (7), band (3) red band, showed the strongest correlation with electrical conductivity, that, as a result, the best type of model was found to be an exponential connection and a regression analysis fitting to tie EC to band 3 (Shrestha, 2006).

Using linear regression to the NDSI, an effective soil salinity model for predicting sugarcane farms Metehara in Ethiopia was established in relation to EC. Other researchers discovered that combining spectral bands from satellite imagery with improved images can be very useful for mapping and modeling soil salinity (Bouaziz et al., 2011). Centered on a moderate resolution imaging spectroradiometer, The Moderate Resolution Imaging Spectroradiometer (MODIS) and linear multiple regression algorithms were used to measure

soil salinity. Researchers have gained significant insight into soil salinity spatial identification owing to the convergence of the Near-Infrared (NIR) (Band 3) with Salinity Index SI2 into a mathematical model (Fallah Shamsi et al., 2013).

As a result, the state of soil salinity and condition is a complex phenomenon that can change over time, particularly in the areas influenced by wind, sand, and drainage conditions. As a result, in such studies, the demonstration that the best stripe set is insufficient for image processing should be taken into account. The goal of this research was to discover the temporal and spatial variation of Salt indications in the soil and to estimate salinity in terms of spectral response to satellite images using digital remote sensing technology and geographic information systems.

By utilizing robust modeling approaches and the data from many remote sensing sources, estimation precision for salt-affected areas has to be increased. Other researchers estimated salt concentrations in soils (electrical conductivity – EC) using the soil backscattering coefficient, groundwater depth (GD), salinity index (SI), and surface evapotranspiration (SET). To provide a scientific basis for increasing soil salinization in this area, the distribution of soil salinity was mapped (Jiang et al., 2019). Researchers have found that utilizing Sentinel 2 pictures, they were able to create successful combined spectral-based statistical regression models to forecast and map regional variation in soil salinity in the Gabes, Hanoch region. (Hihi et al., 2019). With the help of additional researchers, field tests were conducted in the southern portion of Xinjiang Province, China, to validate land with typical alluvial fans and various land uses. Following that, quantitative reflection and numerical mapping on EC using a polychromatic linear tree model and a partial least squares regression model. Furthermore, a cubism model was suggested for achieving high-resolution soil salinity predictions (Peng et al., 2019). Another research used the information from satellite photos and landscape attributes to construct a framework for assessing soil salinity in various settings using machine learning approaches, specifically (Wang et al., 2020).

The goal of the project work was creating a spatial distribution map of salt propagation using GIS, remote sensing, and the points field models from the study region. Observational analysis and evaluation of the existence of salts and their distribution in the study area in order to prepare

them as data and determine the reasons that led to that developing recommendation to the competent authorities for working on implementing geographic information systems to protect agricultural lands from being turned into real estate.

### Location of the study area

The study area was specially defined between longitudes (44°02'0" E) and (44°27'0" E) and two latitudes (31°45'0" N) and (32°03'0" N) due to the low sedimentary plain and the passage of the Euphrates River in its lands Figure 1. It is the most important agricultural area in Al-Diwaniyah.

The Al-Qadisiyah Governorate lands are part of the sedimentary plain of Iraq, it may be identified by its straightforward slope running from the northwest to the south and southeast. Consequently, the contour line (24 m) runs through the Dagharah area, and the line (22 m) through the Al Saniya district, the contour line (21 m) in the city of Al-Diwaniyah, and the line (18.5 m) in the Alasdair district and line (17 m) in Al-Hamzah district, then it falls in the far southeast of the governorate to reach (10 m). Secondary and local variations appear on the governorate surface as a result of a variety of factors, the most significant of which is the process of flood and wind deposition, the nature of which can be explained by dividing the governorate surface into four sections.

To begin, it is represented by the flooding plain, which occupies the majority of the governorate area (90.9%) and is caused by sedimentation brought about by the Euphrates River and

its branches within the study area when floods are present. River shoulders are longitudinal zones that have formed around river sections and forks in the vicinity throughout the river's history, while smaller, finer clay particles accumulated further from river courses to create the Al-Shamiyah river basins. The second part of the surface sections and are distributed in the governorate's northwestern part, which is represented by the remains of marsh Iben Najim in the Levantine district as well as the Abu Balam, Jabour, and Al Yasser marshes in the northwestern part of the Sunni side and the northwestern part. The percentage of this area from the Shafi'i side, in addition to the north-eastern part, which is the Al Dalmaj marsh in Afak district, does not exceed (4.1%) of the governorate area. Because this area has a low surface level, groundwater rises close to the surface. The third section (the dunes area) is located in the southeastern corner of the governorate and is represented by the lands of Afak and Al-Badir sub-districts. The northwest winds played a clear role in transporting sand particles from the surrounding areas, particularly the western plateau, in the form of scattered and unstable dunes, despite the fact that this region accounts for only 1.3% of the total governorate area. The fourth section, which is represented by sandy areas, covers the southwestern part of the governorate, in the area bounded by the west of the Euphrates River and the governorate's western administrative borders, and it is a transitional area between the flood plain and the western plateau, the surface of which is covered with water-soluble gypsum stones, which led to increasement. A summary of the above that the surface of the governorate, despite its altitude variation, is not a hindrance to agricultural activities moving forward, except that surface drainage of surplus irrigation water became challenging due to the lack of a slope, and thus the salinity problem appeared.

### The climate

Al-Diwaniyah's climate is characterized by climate extremes, as temperatures rise in the summer, reaching more than 48.34 degrees in July. The average monthly temperature varies from 26.24 degrees in October to 35.1 degrees in July. During the winter season, the average monthly temperature varies from 11 degrees in January to 17.5 degrees in March. Rainfall in the city of Al-Diwaniyah accounts for the winter

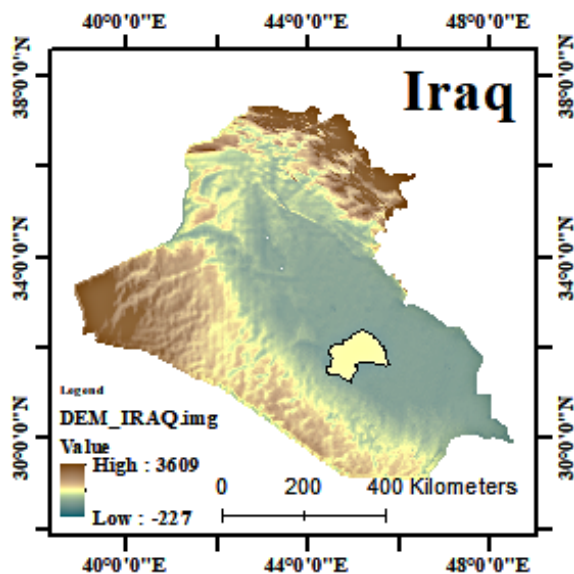


Figure 1. The study area location on a map of Iraq

season, until it peaks in January when the average monthly average is 19.8 mm, then declines until the average in May reaches 5.6 mm, while the summer season is marked by complete drought. C stands for relative humidity. The relative humidity is highest in the winter, at 53.6 percent, and lowest in the summer, at 29.4 percent. The annual rainfall is 3852.6 mm.

## MATERIALS AND METHODS

This section will explain the study area, the procedures and tools used, the data collected to identify and evaluate saline lands in the study area, and the results of the indicators method. Modeling point evaluation, collection, analysis, and spatial distribution using GIS and remote sensing showed in Figure 2, the methodology of this study can be broadly divided into three categories: (1) Electrical conduction field measurements

of EC, (2) Remote sensing data and software, (3) Soil Salinity Indicators (SSI) Figure 3.

## Electrical conduction field measurements of EC

Samples of the soil were taken from the specified points in the drier months at a depth of (0–30) cm in May 2021, the date of the required satellite image. The exact coordinates of each compound were recorded with a 5 m accuracy using (GPS). Each composite soil sample, comprises four soil samples in each composite soil sample subsamples gathered at a 25 m distance in four directions of the central sampling point with a hand drill (19 cm diameter, length 15.2 cm, volume 63.2 cm<sup>3</sup>) which were combined and crushed to create one sample. Twenty samples were chosen based on the spatial representation of the major soil types and the various degrees of salinity. The majority of the points are in deserted areas where salt

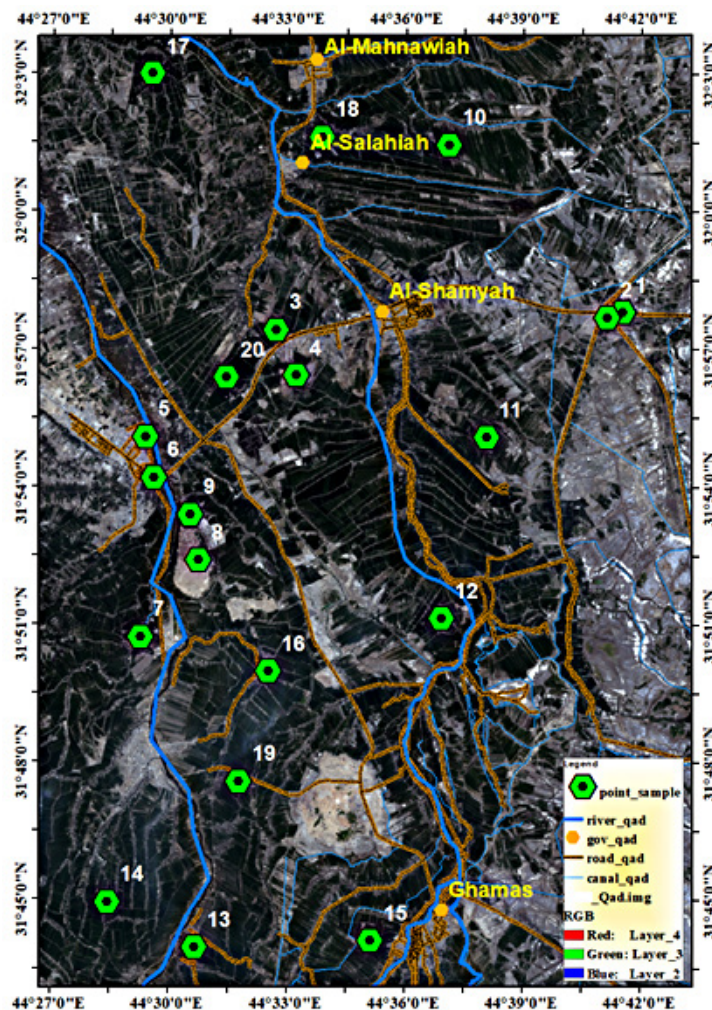


Figure 2. Description of the study area, along with roads, rivers, cities, and sampling points

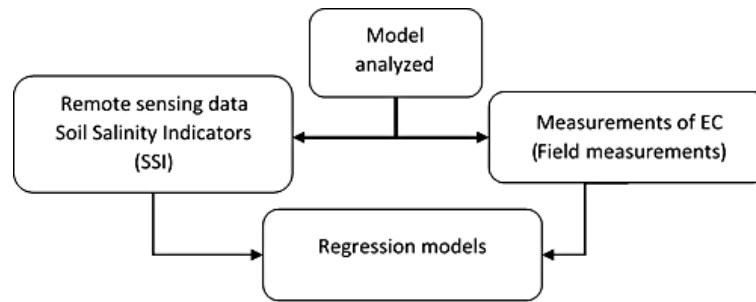


Figure 3. Methodology of the study

accumulation is high. The reason for choosing the coordinates of these points is for several reasons, some of which are green lands in the past and now they are barren lands. Some water drains have stopped working. Surface soil salinity was determined in vitro at 25°C by measuring electrical conductivity. The GPS was used to record the coordinates of each point location. A map of the spatial distribution of soil salinity was created using interpolation techniques.

### Remote sensing data and software

The Landsat 8 satellite's Operational Land Imager (OLI) sensor, obtained in 2021 from USGS Earth Explorer [earthexplorer.usgs.gov](http://earthexplorer.usgs.gov), was detected with an accuracy of 30 meters in this study. When downloading, the image used in this study was systematically corrected. The photograph was taken in 1984 using a Universal Transverse Mercator (UTM) coordinate system, the World Geodetic System (WGS), and area 38. To avoid such problems as seasonal changes, corresponding dates were chosen in accordance with the fieldwork schedules. A desirable May date indicates a lack of clouds with high average salt buildup and surface reflection. Arc GIS 10.2 and the Excel program were used to process the image analysis.

### Soil salinity indicators

In order to accurately detect soil salinity, more than one indicator was used in this study.

Table 1 shows the various indicator formulas for calculating soil salinity. Soil salinity indices (SSI) are primarily used to detect soil salinity based on the spectral responses of saline soils over a wide range of wavelengths. In general, it can be concluded that as soil surface salinity levels rise, so does the spectral response (Schmid et al., 2008). In the presence of salts in the soil, the spectral response varies between the VIS and NIR bands, as well as between the NIR and MIR bands. As a result, these effective ranges must be considered when distinguishing between saline and non-saline soils (Narmada et al., 2015). Where are the following references: Blue, Green, Red, NIR, SWIR1, and SWIR 2 reflecting blue, green, red, semi- infrared, and short waves 1 and 2 in apparent infrared (IR).

## RESULTS

### The relationship between the EC and the salinity indices

Table 2 lists the important statistical parameters for the EC data. According to the Food and Agriculture Organization's (FAO) soil salinity categorization, the EC values in the research region range from extremely highly salty (>16 dS/m), (4–8 dS/m) medium salinity and non-saline (0–2 dS/m). The significant Co-efficient of Variation (CV) of 91.27 percent validates the EC value changes across the research region.

Table 1. Spectral salinity indicators used in this research

Salinity indices	Spectral functions	Reference
Normalized difference vegetation index	$NDVI = \frac{NIR - Red}{NIR + Red}$	Rouse et al., 1973
Normalized differential salinity index	$NDSI = \frac{Red - NIR}{Red + NIR}$	Khan et al., 2005
Salinity index 4	$SI4 = \frac{Red \times NIR}{Green}$	Abbas and Khan, 2007
Salinity index 5	$SI5 = \frac{Green \times Red}{Blue}$	Abbas and Khan, 2007

Approximately 63% of all samples were classed as very salinized soil, indicating the leading class of soil salinity. An association study revealed a substantial correlation is positive ( $p < 0.05$ ) between electrical conductivity and the remote sensed NDVI, NDSI, SI4 and SI5 indices. (Bannari et al., 2008) (Bannari et al., 2008).

### Model selection

Because of its extremely substantial link with EC, the Salinity Index SI4 and SI5 introduced by Abbas and Khan (2007), was utilized to construct improved pictures of soil salinity in this investigation, and at the locations of the sample points over those improved pictures, digital values were retrieved. In selecting the index that generates optimal results for the assessment of salt-affected

regions, it was assumed that the values of the index should be sufficiently two different classes (salt versus non-salt class). In Table 3 the ratio of the indices was used for two adjacent classes, one of which was a non-salt class, to simplify the comparison of different indices. The ratios vary from one Satellite Scene to the next, since the spectral properties of different sites differ from one Satellite to the next. Two types may be employed, as long as the absolute values (NDVI or NDSI), both the standardized differential salinity index (NDSI) and the standard differential vegetation index (NDVI) as shown in Figure 4.

### Model creation and valuation of soil salinity

The multiple linear regression (MLR) method predicts the value of the dependent variable,

**Table 2.** Expressive statistics of measured EC ds/m (electrical conductivity)

Parameter	Min	Max	Mean	SD	CV%
EC	0.01	38	15.56	14.21	91.27

**Table 3.** Correlation linear model coefficient between R squared EC measured ds/m and remotely sensed data

Parameter	NDVI	NDSI	SI4	SI5
EC	42.54%	40.73%	58.23%	70.56%
Equation for the linear model Y: (EC) measured	$Y = 19.85 - 24.34 X$	$Y = 16.44 + 15.34 X$	$Y = - 1.090 + 96.31 X$	$Y = - 2.879 + 110.3 X$

**Note:** significant:  $p < 0.05$ .

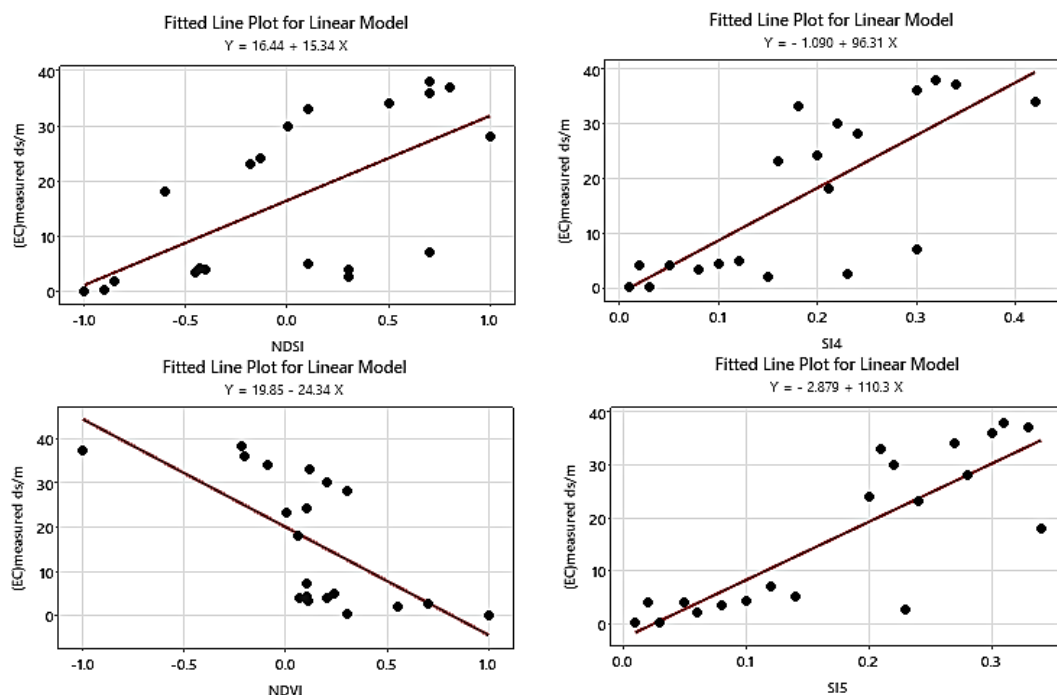


**Figure 4.** Regression for EC measured ds/m vs salinity indices

in this case salinity levels in terms of EC using one or more independent variables. This was accomplished for the successful completion of the responsive domain and index transactions. This model is based on the best salinity indices that have the strongest correlation with EC values (as predictive variables) and EC values from field samples (as response variables). Figure 5 shows the remote sensing for the NDSI, SI4, SI5 and NDVI. Gray background represents an X variable not in the model. The best linear correlations of EC with NDVI and SI5. ( $R^2 = 60.33\%$  and  $R^2 = 89.52$ , respectively) in this paper demonstrated the possibility of predicting soil salinity using

more than one variable (Figure 6). As a consequence, the equation depicts the scientific regression relationship for estimating soil salinity.

### DISCUSSION VALIDATION OF MODELS

The efficiency of the regression analysis of the model’s selection criteria was assessed using the test subset to make sure that they behaved on more than just one set of data, but that accurate results are achieved on other data sets. Table 4 identified two theoretical comparison metrics for the calculated and anticipated values. The  $R^2 = 68.92$  values

**Table 4.** The regression model’s statistical evaluation standards

Coefficient of determination	$\frac{\sum_{i=1}^n (ai - \bar{a})(bi - \bar{b})}{\sqrt{\sum_{i=1}^n (ai - \bar{a})^2 + \sum_{i=1}^n (bi - \bar{b})^2}} \quad (1)$
Root mean square error	$\sqrt{\frac{\sum_{i=1}^n (ai - bi)^2}{n}} \quad (2)$

**Note:**  $ai$  and  $bi$  are values that are measured or predicted;  $\bar{a}$  and  $\bar{b}$  are the means of values that are measured or predicted, and  $n$  is the number of samples.

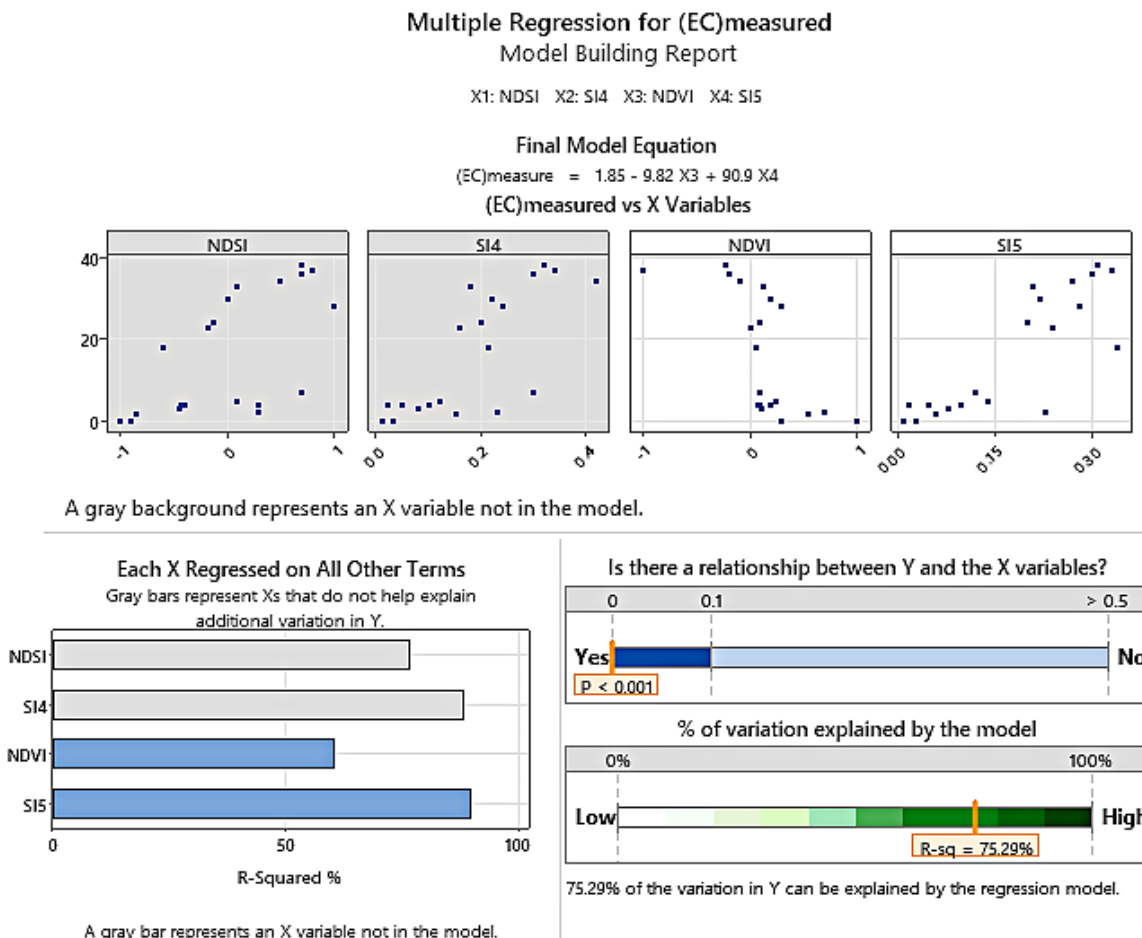


**Figure 5.** Multiple Regression for EC measured and the salinity indices

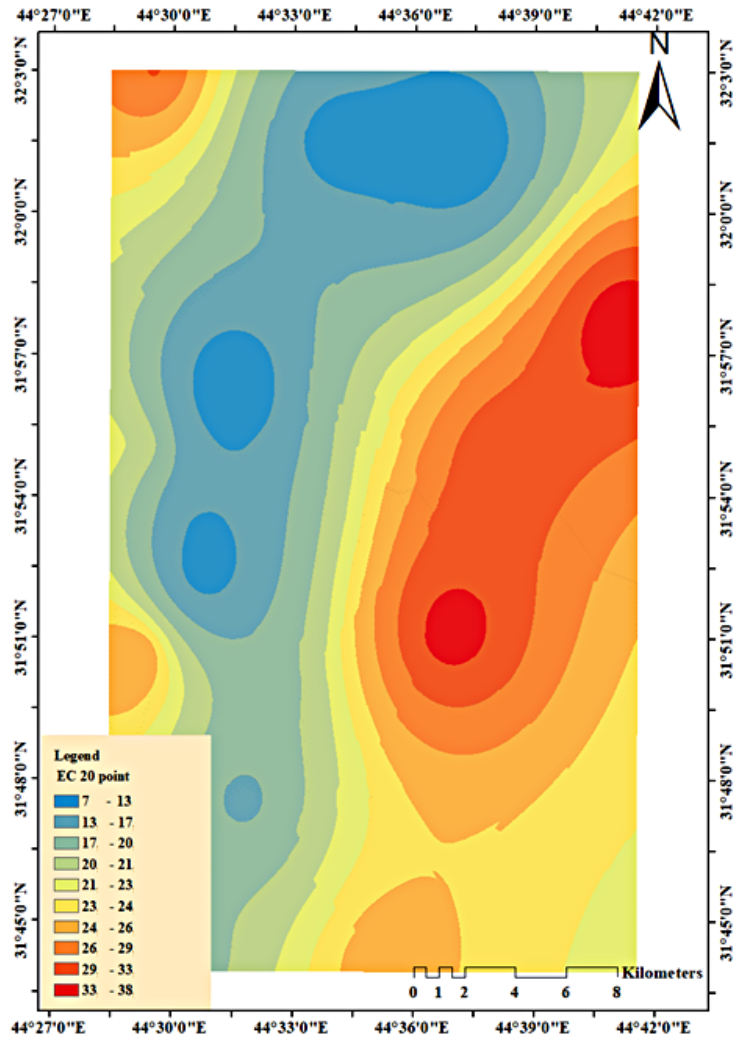


Figure 6. The EC (ds/m) values and their distribution of the 20-point model distributed points

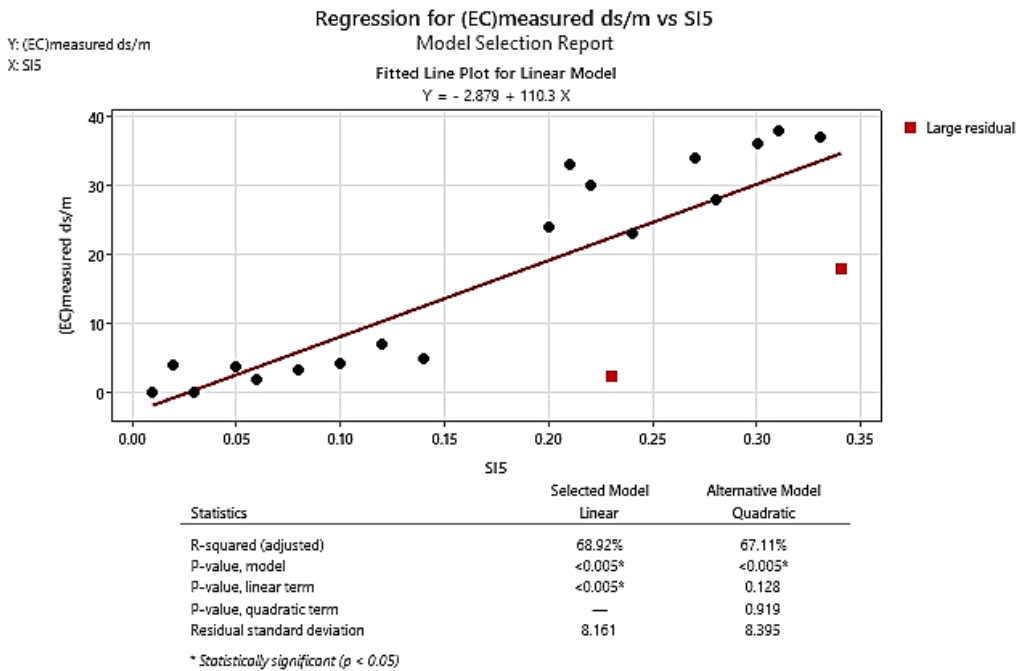
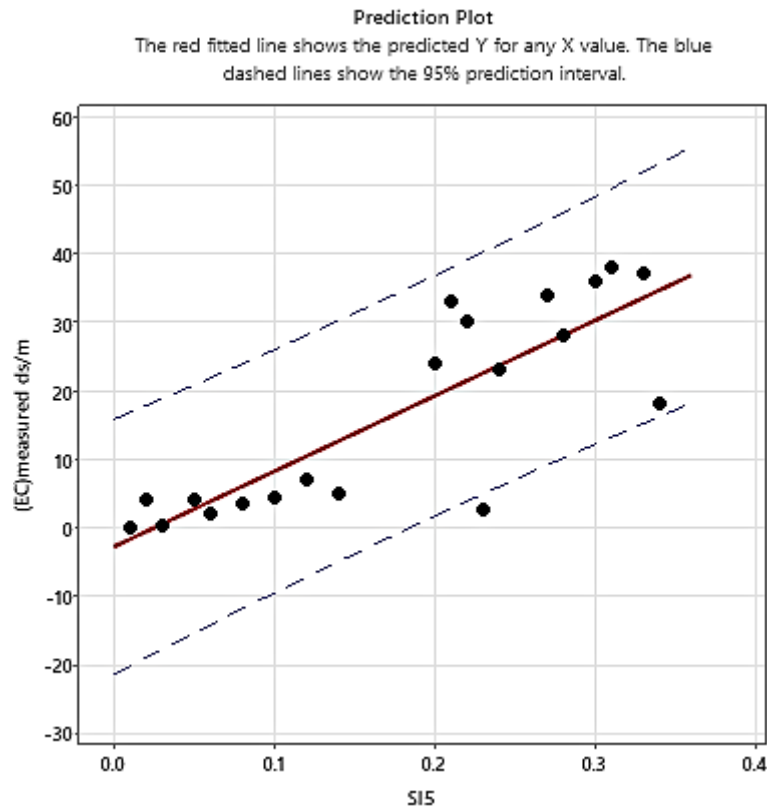


Figure 7. Cross-validation by using regression models, create scatter plots of SI5 vs the observed EC point



**Figure 8.** The anticipated Y for any value of X is shown by the red fitted line. The 95 percent prediction interval is represented by the blue dashed lines

reflect the strength of the statistically linear relation between soil salinity measures and expectations, while Root Mean Square Error (RMSE) represents absolute measurement errors. (Moriassi et al., 2007). Residual standard deviation 8.161 The distribution is normal if the significance level is  $p < 0.05$  or strongly significant: ( $p < 0.005$ ). (‘Discovering statistics using R’, 2012) Table 2 shows the statistical parameters for assessing the regression model shown in Figures 7 and 8.

## CONCLUSIONS

This study aimed to investigate the feasibility of using the Landsat 8 OLI sensor data to discover and map different salinity categories using various soil salinity indicators for a portion of the Al-Diwaniyah Governorate. The combining of these remote-sensing parameters into a single model explained 75.29 percent of the spatial changes in soil salinity there in the study area. The enhanced pictures and red band efficacy in highlighting information from soil salinity account for this combined model’s superiority over previous developed models. Because of its simplicity and

acceptable level of accuracy, the developed model is a suitable tool for future application in soil salinity projection. The findings of this study indicated that the NDSI-based model did not yield sufficient results for certain salinity categories. The findings revealed that the approved SI-4 model was unable to detect the salinity levels of non-elevated and very high saline rows. The model based on (SI-5) was capable of steadily differentiating across all salinity groups while remaining consistent with ground truth measurements. It emphasizes all four major salinity categories. The best-performing indicators were used to build the MLR model, which was then used to predict soil salinity. With a high correlation coefficient ( $R^2 = 68.92$ ), the MLR combining Band 4 and SI-5 was able to discern salinity levels. Finally, it is shown that combining spectral indicators with field measurements can be an effective technique for creating a large-scale chart in predicting and plotting soil salinity.

## Acknowledgments

The authors gratefully acknowledge the Earth Observation Centre, Institute of Climate Change Universiti Kebangsaan Malaysia (UKM), UKM

YSD Chair of Sustainability (UKMYSD-2021-003) and Civil Engineering Department, College of Engineering, University of Al-Qadisiyah, Al-Qadisiyah, Iraq for the support to conduct this study.

## REFERENCES

1. Abbas, A., Khan, S. 2007. Using remote sensing techniques for appraisal of irrigated soil salinity, in: MODSIM07 - Land, Water and Environmental Management: Integrated Systems for Sustainability, Proceedings, 2632–2638.
2. Akramkhanov, A., Vlek, P.L.G. 2012. The assessment of spatial distribution of soil salinity risk using neural network. *Environ. Monit. Assess.*, 184. <https://doi.org/10.1007/s10661-011-2132-5>
3. Bannari, A., Guedon, A.M., El-Harti, A., Cherkaoui, F.Z., El-Ghmari, A. 2008. Characterization of slightly and moderately saline and sodic soils in irrigated agricultural land using simulated data of advanced land imaging (EO-1) sensor. *Commun. Soil Sci. Plant Anal.*, 39, 2795–2811. <https://doi.org/10.1080/00103620802432717>
4. Ben-Dor, E., Goldshleger, N., Mor, E., Mirlas, V., Basson, U. 2008. Combined Active and Passive Remote Sensing Methods for Assessing Soil Salinity, in: *Remote Sensing of Soil Salinization*. <https://doi.org/10.1201/9781420065039.ch12>
5. Bouaziz, M., Matschullat, J., Gloaguen, R. 2011. Improved remote sensing detection of soil salinity from a semi-arid climate in Northeast Brazil. *Comptes Rendus - Geosci.*, 343, 795–803. <https://doi.org/10.1016/j.crte.2011.09.003>
6. *Discovering statistics using R*. 2012. *Choice Rev. Online* 50, 50-2114-50–2114. <https://doi.org/10.5860/choice.50-2114>
7. Douaik, A., van Meirvenne, M., Tóth, T., Serre, M. 2004. Space-time mapping of soil salinity using probabilistic bayesian maximum entropy. *Stoch. Environ. Res. Risk Assess.*, 18, 219–227. <https://doi.org/10.1007/s00477-004-0177-5>
8. Eldeiry, A.A., Garcia, L.A. 2008. Detecting Soil Salinity in Alfalfa Fields using Spatial Modeling and Remote Sensing. *Soil Sci. Soc. Am. J.* 72, 201–211. <https://doi.org/10.2136/sssaj2007.0013>
9. Fallah Shamsi, S.R., Zare, S., Abtahi, S.A. 2013. Soil salinity characteristics using moderate resolution imaging spectroradiometer (MODIS) images and statistical analysis. *Arch. Agron. Soil Sci.* 59. <https://doi.org/10.1080/03650340.2011.646996>
10. Goldshleger, N., Chudnovsky, A., Ben-Binyamin, R. 2013. Predicting salinity in tomato using soil reflectance spectra. *Int. J. Remote Sens.*, 34, 6079–6093. <https://doi.org/10.1080/01431161.2013.793859>
11. Hihi, S., Rabah, Z.B., Bouaziz, M., Chtourou, M.Y., Bouaziz, S. 2019. Prediction of Soil Salinity Using Remote Sensing Tools and Linear Regression Model. *Adv. Remote Sens.*, 8, 77–88. <https://doi.org/10.4236/ars.2019.83005>
12. Jiang, H., Rusuli, Y., Amuti, T., He, Q. 2019. Quantitative assessment of soil salinity using multi-source remote sensing data based on the support vector machine and artificial neural network. *Int. J. Remote Sens.*, 40, 284–306. <https://doi.org/10.1080/01431161.2018.1513180>
13. Jordán, M.M., Navarro-Pedreño, J., García-Sánchez, E., Mateu, J., Juan, P. 2004. Spatial dynamics of soil salinity under arid and semi-arid conditions: Geological and environmental implications. *Environ. Geol.*, 45, 448–456. <https://doi.org/10.1007/s00254-003-0894-y>
14. Lesch, S.M., Strauss, D.J., Rhoades, J.D. 1995. Spatial Prediction of Soil Salinity Using Electromagnetic Induction Techniques: 1. Statistical Prediction Models: A Comparison of Multiple Linear Regression and Cokriging. *Water Resour. Res.*, 31, 373–386. <https://doi.org/10.1029/94WR02179>
15. Liang, J., Ding, J., Wang, J., Wang, F. 2019. Quantitative estimation and mapping of soil salinity in the Ebinur Lake wetland based on VIS-NIR reflectance and Landsat 8 OLI data. *Acta Pedol. Sin.*, 56. <https://doi.org/10.11766/trxb201805070182>
16. Malins, D., Metternicht, G. 2006. Assessing the spatial extent of dryland salinity through fuzzy modeling. *Ecol. Modell.*, 193, 387–411. <https://doi.org/10.1016/j.ecolmodel.2005.08.044>
17. Minasny, B., McBratney, A.B. 2016. Digital soil mapping: A brief history and some lessons. *Geoderma*, 264, 301–311. <https://doi.org/10.1016/j.geoderma.2015.07.017>
18. Moriasi, D.N., Arnold, J.G., Van Liew, M.W., Bingner, R.L., Harmel, R.D., Veith, T.L. 2007. Model Evaluation Guidelines for Systematic Quantification of Accuracy in Watershed Simulations. *Trans. ASABE*, 50, 885–900. <https://doi.org/10.13031/2013.23153>
19. Peng, J., Biswas, A., Jiang, Q., Zhao, R., Hu, J., Hu, B., Shi, Z. 2019. Estimating soil salinity from remote sensing and terrain data in southern Xinjiang Province, China. *Geoderma*, 337, 1309–1319. <https://doi.org/10.1016/j.geoderma.2018.08.006>
20. Qu, Y., Jiao, S., Lin, X. 2008. A partial least square regression method to quantitatively retrieve soil salinity using hyper-spectral reflectance data, in: *Geoinformatics 2008 and Joint Conference on GIS and Built Environment: Classification of Remote Sensing Images*, 71471H. <https://doi.org/10.1117/12.813254>
21. Salinity: Environment - Plants - Molecules, 2004., Salinity: Environment - Plants

- *Molecules*. Dordrecht, The Netherlands. <https://doi.org/10.1007/0-306-48155-3>
22. Shrestha, R.P. 2006. Relating soil electrical conductivity to remote sensing and other soil properties for assessing soil salinity in northeast Thailand. *L. Degrad. Dev.*, 17, 677–689. <https://doi.org/10.1002/ldr.752>
23. Taghizadeh-Mehrjardi, R., Minasny, B., Sarmadian, F., Malone, B.P. 2014. Digital mapping of soil salinity in ardakan region, central iran. *Geoderma*, 213, 15–28. <https://doi.org/10.1016/j.geoderma.2013.07.020>
24. Wang, J., Ding, J., Yu, D., Teng, D., He, B., Chen, X., Ge, X., Zhang, Z., Wang, Y., Yang, X., Shi, T., Su, F. 2020. Machine learning-based detection of soil salinity in an arid desert region, Northwest China: A comparison between Landsat-8 OLI and Sentinel-2 MSI. *Sci. Total Environ.*, 707. <https://doi.org/10.1016/j.scitotenv.2019.136092>
25. Wang, N., Xue, J., Peng, J., Biswas, A., He, Y., Shi, Z. 2020. Integrating remote sensing and landscape characteristics to estimate soil salinity using machine learning methods: A case study from southern xinjiang, china. *Remote Sens.*, 12, 1–21. <https://doi.org/10.3390/rs12244118>